

Integration of Borehole and Seismic Data into Magnetotelluric Inversion: Case Study over the Kevitsa Ultramafic Intrusion, Northern Finland

Kieu, D.T.^[1], Kepic, A.^[1], Le, C.V.A.^[1]

1. Deep Exploration Technologies CRC and Curtin University

ABSTRACT

Inverse magnetotelluric (MT) problems are nearly always non-unique. Typically, a smoothness criterion is added to the earth model to produce a stable solution. However, this process tends to produce unrealistic geological models. In reality, the subsurface geology tends to be composed of distinct rock units that are better defined by sharp boundaries rather than diffuse or smooth boundaries. Thus, inversion algorithms that can build an earth model with groups relating rock units should be more accurate. We present the application of fuzzy clustering as an added constraint within the inversion process to guide model updates toward earth models that may resemble geological units. Moreover, fuzzy clustering enables the inclusion of additional prior information from boreholes, such as geochemistry and petrophysics, into the inversion process. The integration of this extra information produces geo-electrical distributions that fit measured MT data and simultaneously honour the prior information from boreholes better. The synthetic examples demonstrate that by adding an extra constraint using fuzzy clustering recovers the true model better than using a smooth constraint. Additionally, fuzzy clustering provides a flexible and robust mechanism to include prior petrophysical and spatial information to build seed models that are closer to the true model. We have applied this technique to the case study of the Kevitsa deposit within the Kevitsa ultramafic intrusion in northern Finland. The geological structure in this area is complex, but the physical properties of the units are reasonably well defined. In this case, the spatial distribution of conductivity is not smooth; therefore, inversion of the MT data with smooth constraints only will not produce a representative or accurate model. In contrast, our algorithm resolves these issues by using fuzzy clustering techniques that build the model comprising units; plus it allows additional borehole data to assist in constructing the units more reliably during the inversion process. A key contribution of our work is to fully exploit borehole data by including both petrophysical properties and other geo-spatial information to constrain the inversion. Finally, a combination of MT inversion and seismic acoustic impedance is put into the fuzzy clustering technique to generate a 'pseudo-lithology' image from the final cluster model as an aid to geological interpretation.

INTRODUCTION

The magnetotelluric (MT) method is a well-known method to map the electrical conductivity of the subsurface that is particularly known for deep crustal studies. MT for the exploration of minerals is becoming more common as it can map mineralized zones at considerable depths without heavy equipment. However, the inversion of MT data is ill-posed. To deal with this issue, smoothness criteria are added to constrain the inversion solutions (deGroot-Hedlin and Constable, 1990). Consequently, the smoothest model is chosen, resulting in unrealistic geological models as few geological boundaries tend to be as vague and diffuse as the smooth models. In geology, the subsurface is usually divided into distinct rock units. Typical subsurface structures in crystalline rock consist of geological units of similar properties. Thus model construction is more reliable if grouping criteria are added to constrain the inversion process. We propose to exploit the robustness of the fuzzy c-means (FCM) clustering techniques (Bezdek et al., 1984) to constrain the MT inversion routine (Sun and Li, 2011) so that conductivity models with "clustered" conductivity distributions are favoured.

The MT method is based upon diffusive fields as it utilizes low-frequency electromagnetic waves. Therefore, the method loses resolution and 'sharpness' with depth. Moreover, the intrinsic difficulty with MT inversion is that multiple models of conductivity can generate an indistinguishable electromagnetic

signature. In order to reduce the ambiguity and to increase model resolution and boundary 'sharpness', extra information from other sources is needed, which comprise spatial and petrophysical information. Li and Oldenburg (2000) reported that the structural constraints such as geological information could build a better model. The petrophysical constraints using borehole data also improve inversion results. The borehole data can be utilized in the inversion constraints as a reference model (Farquharson et al., 2008) or statistical models (Johnson et al., 2007; Sun and Li, 2011). It is usually better if both structural and petrophysical constraints are exploited (Lelièvre et al., 2009; Kieu et al., 2016b). However, the structural constraints can work well in a simpler structural environment, such as sediment layers. It costs time to extract structural information from a complex media such as the crystallized "hard rock" environment, and this information usually comes from a subjective interpretation process. The borehole data most likely represents reliable information. But, this information is usually localised and often only partly available in the area of interest. For example, the boreholes are only valuable to their depth of penetration, and the properties of the inverted model may not be acquired. Consequently, the use of borehole data to build reference models or to form statistical models may not fully exploit this data.

In this study, we propose the use of fuzzy clustering in the inversion. Our strategy can automatically extract borehole information to put in the inversion, and is applicable even where the borehole attribute differs from the model parameter. The

fuzzy cluster constraint enhances the accuracy of the entire model because even away from the boreholes the models tend to use values similar to the “known values”. We utilize lithological information, assay and petrophysical data from boreholes to assist the MT inversion process in building more “blocky” models via clustering analysis. The resultant model must fit the MT data and also honor the extra borehole information, which need not be restricted to electrical conductivity constraints.

The inverted models of MT are usually compared to the interpreted results of other geophysical imaging methods that map the geological subsurface. For example, MT models can be evaluated by referring to seismic features because the seismic method has a higher resolution than the MT method. However, the resistivity model may differ from the seismic model; and the combination of multiple models usually produces better geological images than a single model (Paasche et al., 2006; Ogaya et al., 2016). In this work, the final MT model is compared with the acoustic impedance model, and then the two models are used as input data for FCM clustering. The output (result) is a cluster model that can greatly aid the geologic interpretation process.

METHODOLOGY

Fuzzy c-means Clustering

The Fuzzy c-means (FCM) clustering algorithm (Bezdek et al., 1984) is an unsupervised learning method that defines clusters of items based on similarities by minimization of the weighted error between the elements of the dataset and the centre or prototypes values. The objective function of the algorithm is described as following:

$$\Phi_{FCM} = \sum_{j=1}^N \sum_{k=1}^C u_{jk}^q \|z_j - v_k\|_2^2 \quad (1)$$

where N and C are the number of data z_j ($j=1, \dots, N$) and cluster number, respectively. q is the fuzziness parameter, $q > 1$, in this study q is set to equal 2, a value widely used (Sun and Li, 2011). v_k is the centre value of the k th cluster, and u_{jk} is the membership degree, with the constraint $\sum_{k=1}^C u_{jk} = 1$. The FCM objective function corresponds to a weighted sum of errors (or distance) when replacing data set, \mathbf{Z} ($z_j, j=1 \dots N$), by centre values, \mathbf{V} ($v_k, k=1, \dots, C$).

In this study, FCM is utilized to analyze the borehole data (Kieu et al., 2015) and to constrain the inversion process (Kieu et al., 2016a; Kieu et al., 2016b). In our inversion routine, FCM plays a two-fold role: first, it is an extra constraint in the inversion to partition the model into clusters that may reflect rock units; secondly, it is a platform to include other prior information, such as borehole elemental analysis data, into the inversion process.

Inversion Algorithm

Our inversion algorithm is formulated with the least-squares minimization of the following objective function (Sun and Li, 2011, Kieu et al., 2016b):

$$\Phi = \Phi_d + \beta \Phi_m + \gamma \Phi_{FCM}, \quad (2)$$

where Φ_d measures the difference between observed data and synthetic data from the inverted models, Φ_m represents the smoothness constraint and Φ_{FCM} is the FCM objective function (equation 1). This “model guider” term directs the model updating process. More specifically, it drives the incorporation of rock units within the inverted model. The regularization parameters β and γ balance between misfit, model structure and FCM constraint terms. The prior information is included in the inversion routine via FCM (Kieu and Kopic, 2015; Kieu et al., 2016b).

The prior petrophysical representative values are included in the inversion routine via FCM (Kieu et al., 2016a; Kieu et al., 2016b). During the inversion process, FCM clustering classifies N samples of the model \mathbf{Z} ($z_j, j=1, \dots, N$) into C subsets based on feature similarities. The clustering process drives the group central value \mathbf{V} ($v_k, k=1, \dots, C$) towards the prior representative conductivity \mathbf{P} ($p_k, k=1, \dots, C$). The objective function of FCM is modified from equation (1) to equation (3).

$$\Phi_{FCM} = (1 - \eta) \sum_{j=1}^N \sum_{k=1}^C u_{jk}^q \|z_j - v_k\|_2^2 + \eta \sum_{k=1}^C \|p_k - v_k\|_2^2 \quad (3)$$

η is the weighting value that represents the confidence level of the prior information. In this work, we set this value to 0.5 for both synthetic and real examples.

To integrate boundary information within the inversion via FCM, the boundary information \mathbf{b} is combined with the model parameter \mathbf{m} to form the data input $\mathbf{Z} = [\mathbf{m} \ \mathbf{b}]$ of the FCM clustering process (Kieu et al., 2016b).

EXAMPLES

Synthetic Data

A synthetic model (Figure 1a), which is the same as one used by Lee et al. (2009) and Sasaki (1989), includes a conductive layer of 5 Ωm superimposed on the host media of 50 Ωm . The layer is interrupted and off-set at a fault between the 9th and 11th km along the profile. Near the surface, there are two resistive and conductive objects of 100 Ωm and 10 Ωm . MT stations are located every 1 km from 0 to 20 km along the profile. The frequency band is the same in Lee et al. (2009) which is 0.10, 0.22, 0.50, 1.00, 2.20, 5.00, 10.00, 22.00 and 50.00 Hz. The synthetic data is generated by the MT forward modelling code Lee et al. (2009) plus 5% Gaussian random noise.

First, we run the MT inversion with the same set up as in the work of Lee et al. (2009). The 2D inverted model is presented in Figure 1b. The result matches the true model. However, the boundaries are blurred because of the smoothness constraint. The inverted model values are distributed relatively evenly in a wide range from smallest to the highest values of the true model (Figure 3a).

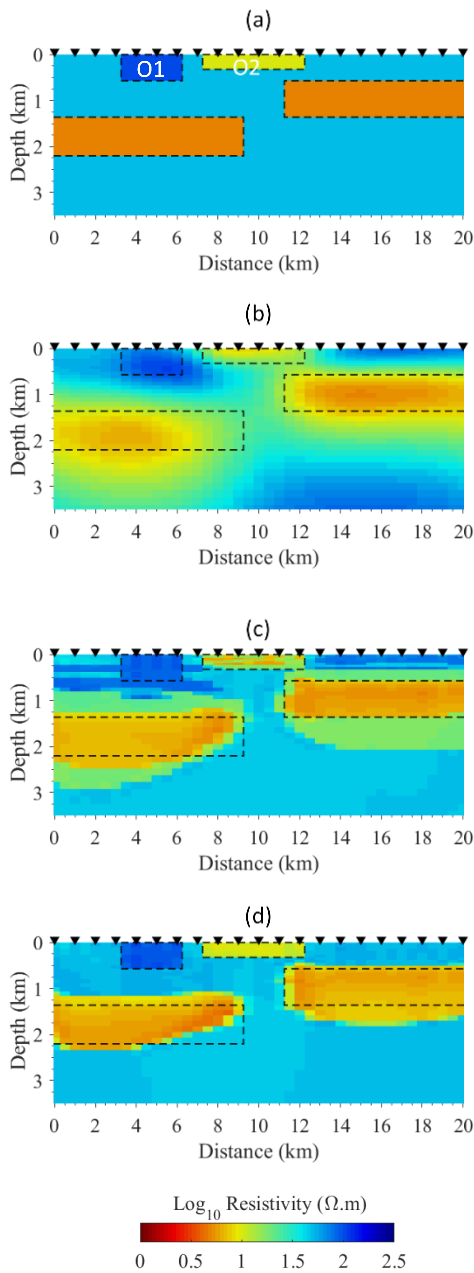


Figure 1: Comparison between our inversion results (c) and (d) with the published model (b) (Lee et al., 2009) from synthetic data generated by a model (a). The dashed lines mark the boundaries of the true model. The triangles on the top of the sections mark the position of MT stations. Our result recovers distinct boundaries better than the typical smooth inversion result. In our inversion, we include additional constraints: petrophysical constraints for cluster centres (c) and the approximate boundaries of the objects O1 and O2 (d).

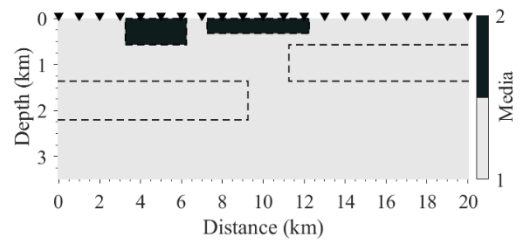


Figure 2: Prior boundaries of the two objects at shallow depth, O1 and O2 (Figure 1a) separating the earth model into two media (clusters) is used as a constraint in the MT inversion. This ensures that models that have similar structures and fit the data are most likely to emerge.

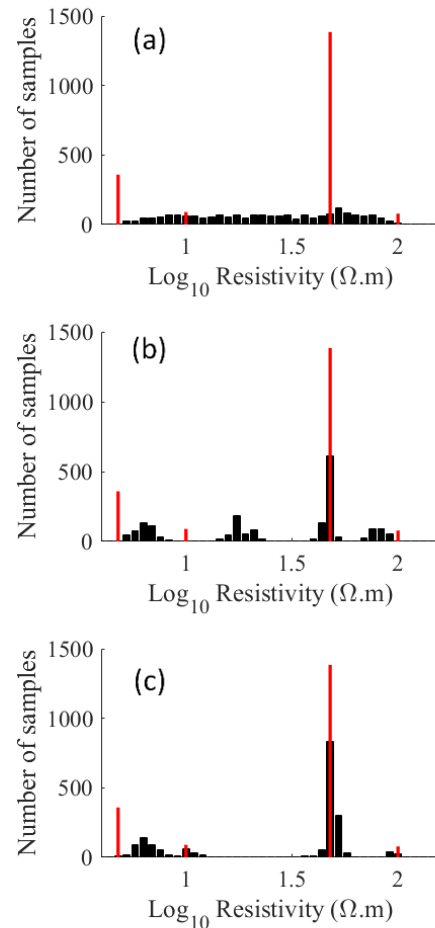


Figure 3: Histogram of the inverted models using different constraints: (a) Smoothness constraint; (b) Smoothness and petrophysical constraint; (c) the same constraint as in (b) plus the boundaries of the shallow objects. The inversion with extra information recovers the model values better than using a smoothness constraint only. The red bars show the true model.

We have modified the 2D MT inversion code from Lee et al. (2009) whilst retaining the original forward solution. An inversion is performed with the synthetic data for two cases:

- i. The typical petrophysical values of the media (i.e., the centre values $\mathbf{P} = [5; 10; 50; 100] \Omega\text{m}$ is included
- ii. Boundary information of the two shallow objects is available (Figure 2) as a “soft” constraint.

This procedure is the same as that used by Kieu et al. (2016b). The same regularisation parameters β and γ are used for both cases. The initial model is set to a homogeneous value of 15 Ωm . These synthetic models test how FCM can improve the MT inversion. More importantly, it shows that if we know the boundaries of shallow objects, information that is usually available for mining projects, it improves the whole model considerably.

When petrophysical information is included in the clustering definition of the inversion process, the result (Figure 1c) matches well with the true model. In comparison with using a smoothness constraint, it removes the artefact at the bottom right corner of the section. Also, the lower conductive slabs are better defined. The distribution of values of the inverted model (Figure 3b) are more consistent with the true distribution than the values from the smooth inversion (Figure 3a).

If boundary information of the two shallow objects O1 and O2 (Figure 1a) is available (for example from drilling), then we can divide the section into the two media (Figure 2) as both, a starting model and as a constraint. This information is incorporated into the inversion process via a localised cluster constraint: pick any cluster as long as it is “this one”. As we are concerned about the boundary location rather than the conductivity, it means that we can include different data, for example, assay or other physical data to select a cluster boundary. The inversion result (Figure 1d) nearly recovers the true model. Also, the conductivity values (Figure 3c), are closer to the true values than just using petrophysical constraints, and much better than inversion with a smoothness constraint.

These synthetic examples demonstrate the power of being able to direct the inversion algorithm to pick a limited number of petrophysical properties to construct a model. Such direction also leads to a model that is more representative and interpretable for mineral exploration.

Application to Real Data

We have selected the Kevitsa data set as a test site because it is unusually rich in borehole petrophysics, has both MT and 3D seismic reflection surveys to relate boundaries at depth with, and much of the information is in the public domain. The dataset was acquired at the Kevitsa Ni-Cu-PGE deposit within the Kevitsa ultramafic intrusion in northern Finland (Figure 4a). The MT profile includes 48 stations (Figure 1b), the period ranges from 0.0001 to 1s. The borehole data shows that this area can be divided into conductive and resistive environments (Figure).

Conductive zones may relate to ore zones or/and carbonaceous phyllite.

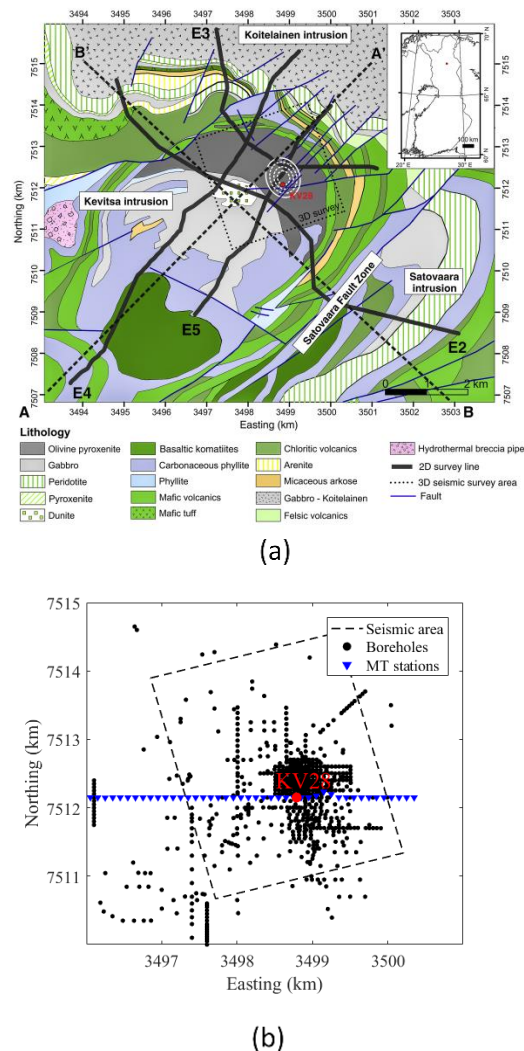


Figure 4: (a) Geological map adapted from Malehmir et al. (2012). (b) Location of MT stations, 3D seismic survey area and boreholes. The bold red dot marks the location of borehole KV28 that is used to validate the processing data. Note that assay data was acquired in almost all holes in this area, but the wireline logs of resistivity are only available in a limited number of the holes. That is the reason why we integrate assay data into the MT inversion instead of resistivity.

Borehole Data Analysis

A histogram of the borehole resistivity data (Figure 5) illustrates that a conductive model of the subsurface in this area is well separated. The conductive media may relate to mineralized zones and/or carbonaceous phyllite, and the remaining rocks are resistive. The borehole data shows that rocks in this area tend to have a bi-modal distribution of values in resistivity, which is difficult for an inversion with a smoothness constraint to effectively reproduce.

In order to integrate borehole information directly into the inversion process, we need to investigate the relationships between resistivity and other borehole-derived properties. The correlation between physical properties and assay data is poor (Steel, 2011). Figure 6 shows that the linear correlation between resistivity and other properties in borehole KV28 is not high. The best correlated measurements are between resistivity and Co with a correlation coefficient value of -0.54. The correlation of resistivity and density is small, and it is worse than with P-wave velocity. That is problematic if we try to use these borehole properties as conventional local constraints in the inversion process.

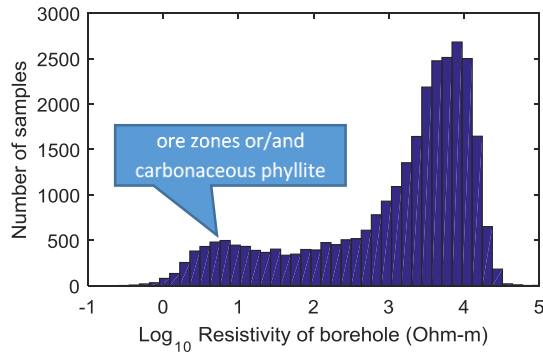


Figure 5: Histogram of resistivity of the borehole data shows two main geoelectrical environments. These are resistive rocks and conductive media relating to the ore zones and carbonaceous phyllite.

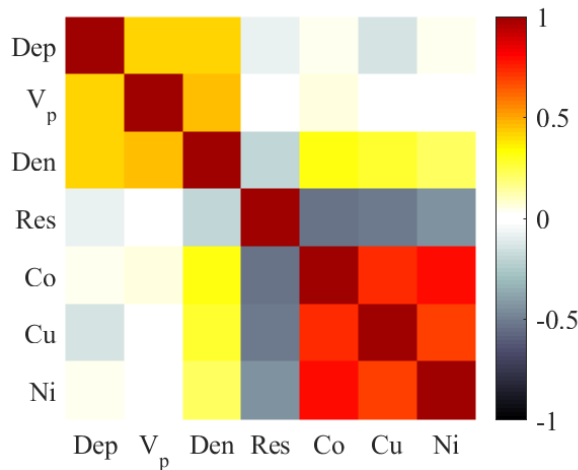


Figure 6: Correlation matrix of the borehole data in KV28. There is no strong correlation between resistivity and assay data, nor between resistivity and the other petrophysical properties. Abbreviation: Dep - depth; V_p - P-wave velocity; Den - density; Res - resistivity; Co – cobalt; Cu – copper; Ni - nickel.

In our process, we use FCM clustering to form relationships between various properties. The basic idea of clustering is to separate items (local cells) into groups, the variation of an item value is used to place the item in a different group, rather than directly define the values of the items. To compare the variation

of resistivity and other features of the hole KV28, the variation of the data is calculated such that:

$$Variation = \left(\frac{data - mean(data)}{mean(data)} \right)^2 \quad (5)$$

Figure 7 presents the standardized values of the variation of resistivity, acoustic impedance, Cu and Ni. These values show a reasonable correlation and are consistent along the length of the borehole.

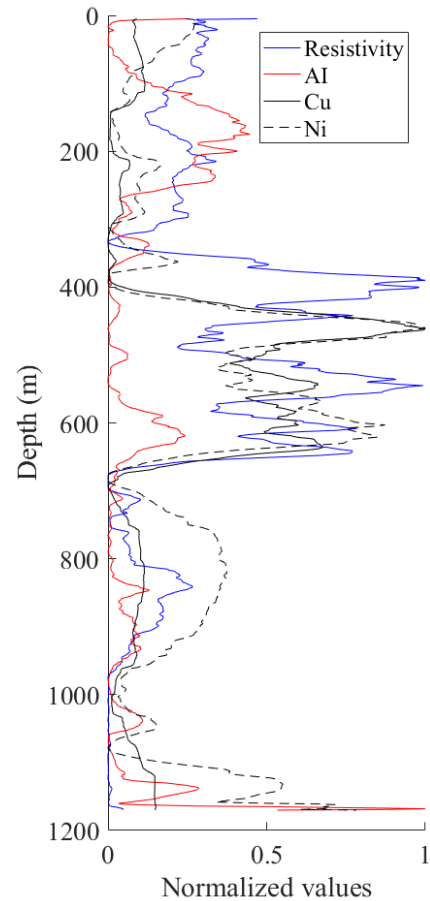


Figure 7: Normalized variation values of resistivity, acoustic impedance (AI), Cu and Ni in borehole KV28. First the variation of the data is calculated (Equation 5) then normalized to the range [0, 1].

Note that in our synthetic inversion example, when we include boundary information of the two shallow objects, we were only concerned about the variation of the inverted physical property. In the Kevitsa data, we have reasonable correlations between the various measured properties. That means we can incorporate assay data to help define the clusters in the inversion of MT data.

The next issue is how to include the rather localised borehole data to be used across the whole model of MT. We assume that the properties of each cell in the MT model mesh should be similar to the nearest borehole samples with a level of certainty.

In this work we weigh this certainty according to the following formula:

$$Certainty = \exp\left(-\frac{d}{\alpha}\right) \quad (6)$$

where d is the distance from a borehole to the MT section, α is a scaling factor that controls the radius of influence of borehole data to the vicinity. Figure 8 displays the “certainty” of projected borehole data on the MT section.

In the next step, we cluster the Co, Cu and Ni assay data from all holes, and project the interpolated cluster map onto the MT section (Figure 9). This information is then integrated into the inversion process as before with boundary information in the synthetic example. However, in this case, we incorporate the certainty weighting.

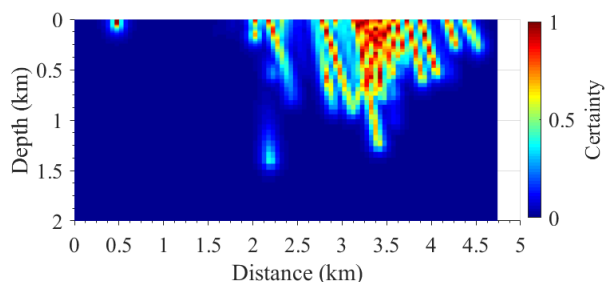


Figure 8: The borehole certainty weights projected on the MT section. The certainty is calculated by the distance from borehole to the section (Equation 6).

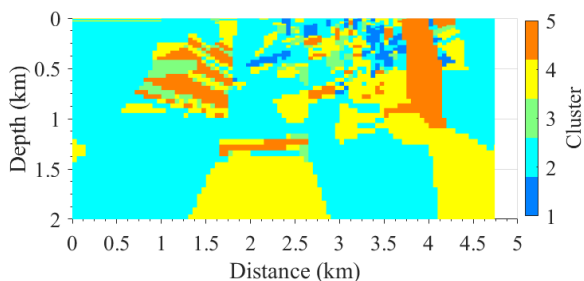


Figure 9: Clustering and extrapolation results of borehole assay data, including Co, Cu and Ni, projected on the MT section.

Inversion of Kevitsa MT Data

We have run the inversion of the MT data with a traditional inversion algorithm, ModEm code (Egbert and Kelbert, 2012); hereafter this inversion result is referred to as “Inv. ModEm” (Figure 10a). It detects the mineralization confirmed by many holes. However, it also appears to create a significant artefact in the right bottom corner of the section, and more importantly, it shows a resistive zone (zone B) where borehole data shows a significant conductive zone.

Our FCM inversion process is run with two scenarios. First, just statistical information from boreholes is included, and second,

we integrate the cluster information directly from boreholes into the inversion. Hereafter, we name the two inversion strategies Inv. FCM and Inv. FCM+BH, respectively. The inversion starts with a homogeneous initial model of 600 Ωm , an average value based on borehole data. We run our inversion routine with different numbers of clusters plus using cluster analysis on available borehole data; only the results from using five clusters are shown here. All other inversion parameters (such as the LSQ misfit and prior weighting) are set identically for the two cases.

Discussion

Our synthetic tests demonstrate that petrophysical constraints via FCM clustering perform better than using a smoothness constraint. Moreover, using known shallow boundaries improves the inversion greatly. This scenario is very common in practical conditions where we often have information on the near-surface, and our objective is to know what is happening at greater depths. This encouraged us to trial the approach with Kevitsa.

Figure 10b and c show, respectively, the inversion results of the two scenarios Inv. FCM and Inv. FCM+BH. First, initial values of FCM clustering of the borehole data is included in the inversion process. In this strategy, the program drives the model to produce conductivities with centre values similar to cluster centre values from the borehole data. Second, the clustering of borehole data is projected on the entire MT section and included into the inversion process in the same manner as with boundary information; in this case, the cluster label is the same as the “media” label in the previous synthetic example. As mentioned previously each cell’s certainty weighting is incorporated into the inversion to allow prior borehole data to influence the result.

Both of our FCM inversion results detect the mineralization (zone A) and are more consistent with borehole data than Inv. ModEm. The conductive zone B that is confirmed by the borehole data appears in both inversion results. The main differences between the two models are that resistive zone C and conductive zone D are more evident in the model of Inv. FCM+BH than in the model of Inv. FCM. Also, neither of our models have a very conductive near-vertical feature in the basement under zone A.

We have applied our FCM inversion strategies to real data from the Kevitsa mine site, where there is a wealth of information from many boreholes and seismic reflection data. However, there are no deep boreholes in this area, and the quality of the seismic reflection data is not sufficient for robust impedance inversion, particularly at great depths because of a low signal-to-noise ratio. Thus, the MT method can provide an additional tool to image the subsurface at greater depths. In comparison with a traditional inversion algorithm ModEm code (Egbert and Kelbert, 2012) that uses only smoothness constraints, our algorithm constructs distinct resistivity zones that reflect the true rock units.

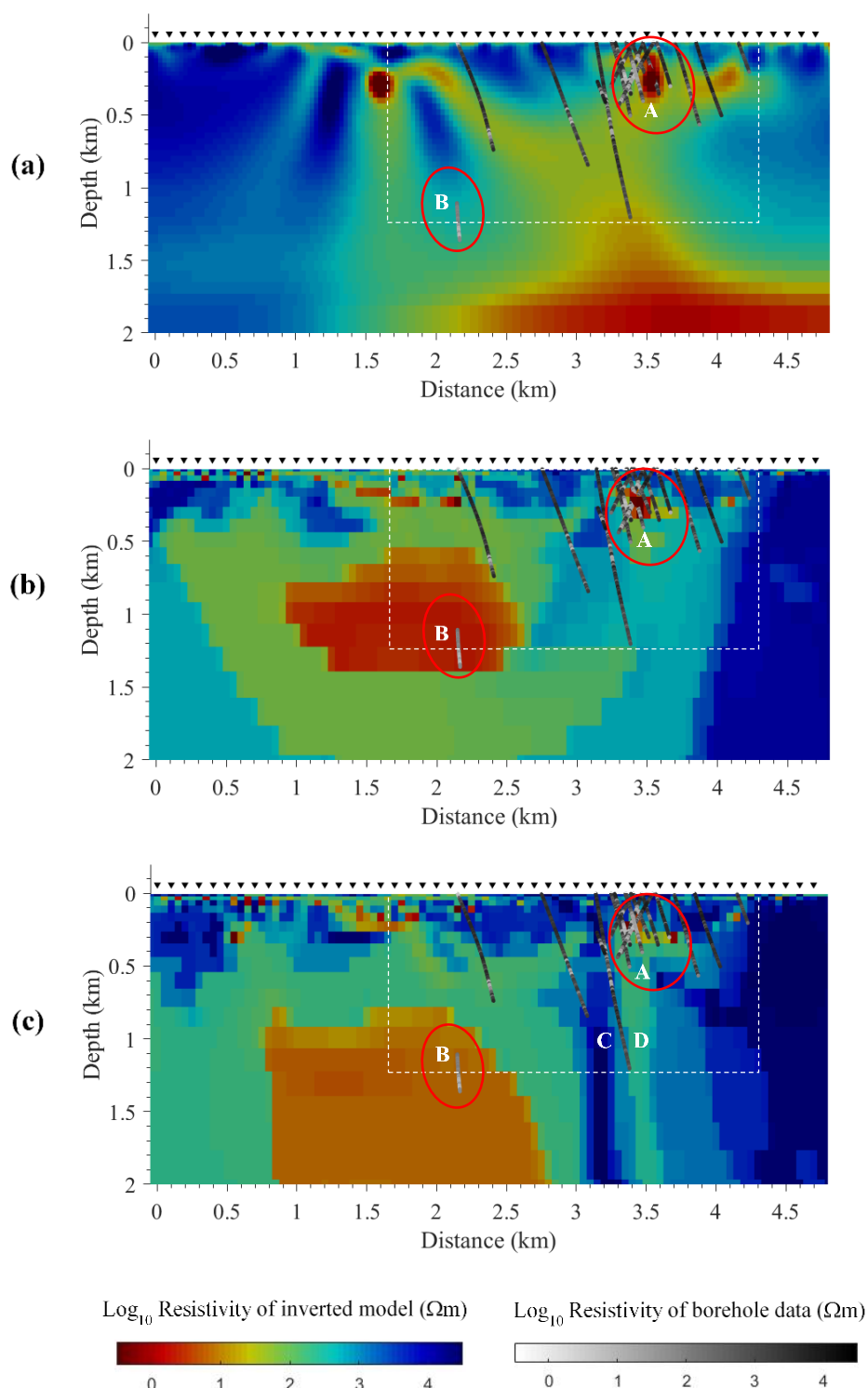


Figure 10: Inversion results of the MT line using different constraints: (a) Inv. ModEm using a smoothness constraint (Egbert and Kelbert, 2012); (b) Inv. FCM using petrophysical distribution constraints; (c) Inv. FCM + BH using petrophysical statistics to guide cluster centres, and the integration of assay data to constrain which particular cluster to weight towards. The boreholes (grey scale) in 100 m vicinity of the MT profile are projected on MT model to compare with inverted models (jet colour scale). The triangles at the top of profile mark locations of MT stations on the profile. The dashed white line shows the area mapped with 3D seismic data. The red circles mark conductive zones, the shallow zone is ore body.

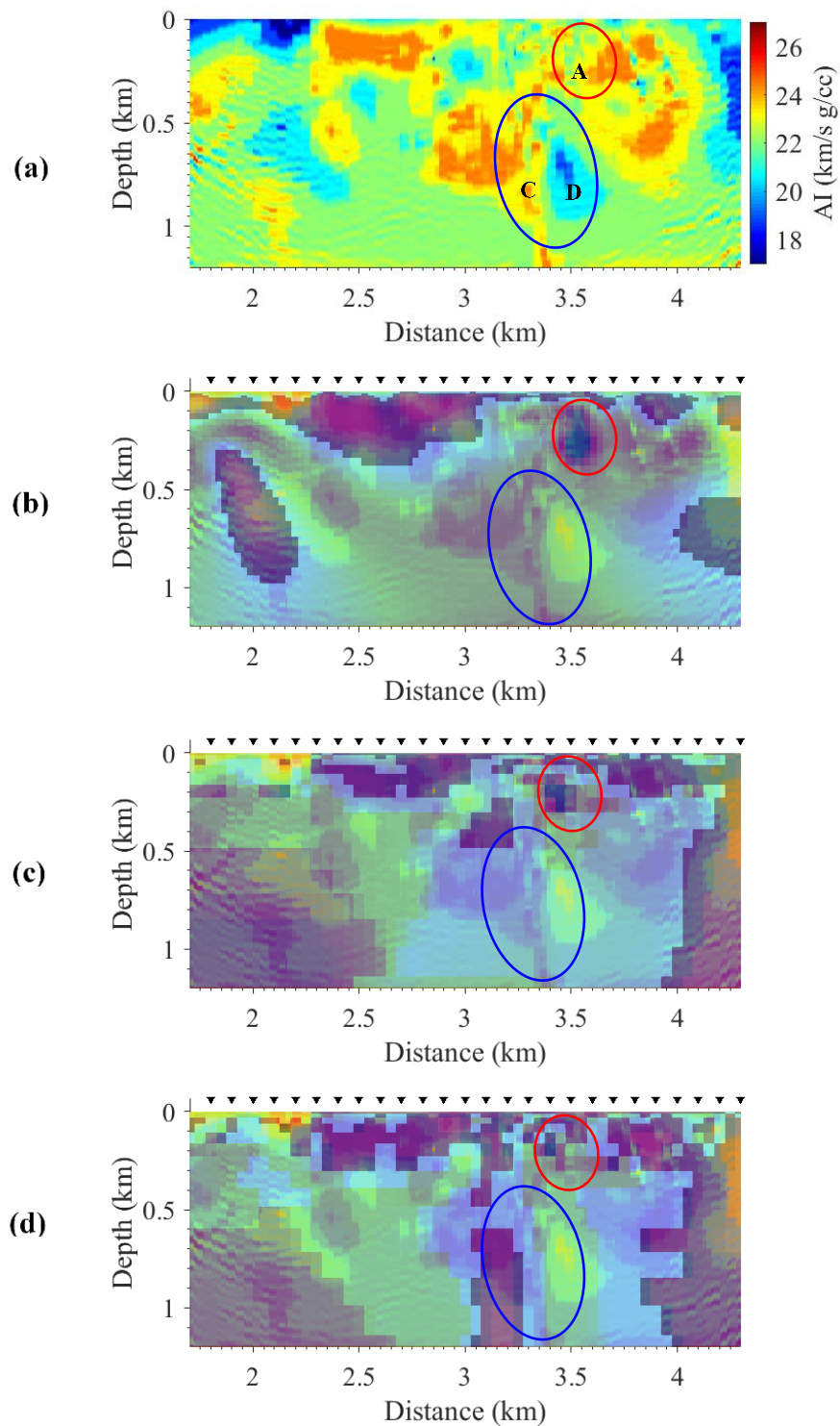


Figure 11: (a) Section of acoustic impedance (AI) generated via model-based inversion of seismic reflection data. Overlay of AI and inverted MT models: Inv. ModEm (b); Inv. FCM (c); Inv. FCM + BH (d). The red circles show position of the Kevitsa orebody (zone A), blue circles mark zone C and D positions. Note that these sections are cropped from the sections in **Error! Reference source not found**.Figure 10 (marked by dashed white rectangles).

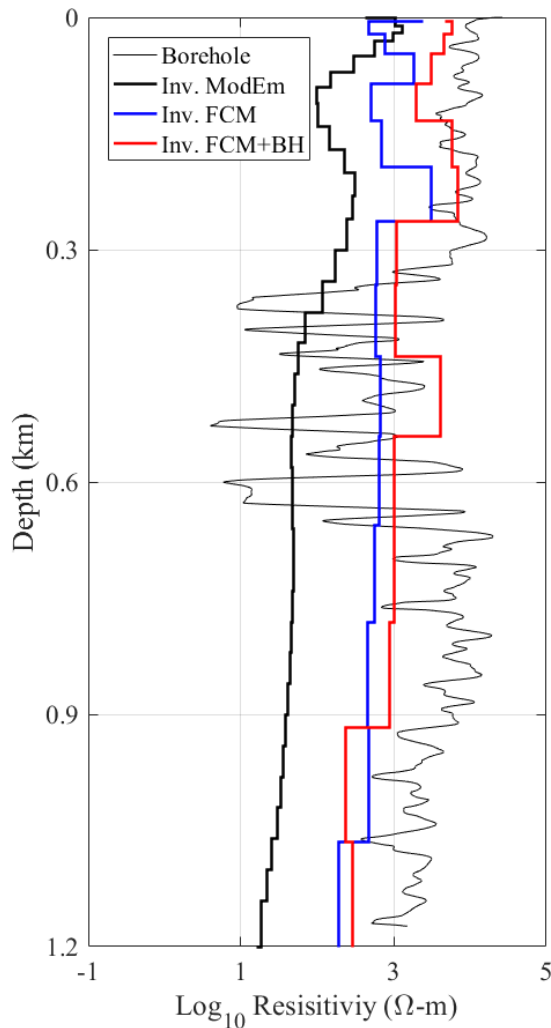


Figure 12: Comparison between data from borehole KV28 and inversion results using ModEm code (Inv. ModEm), our program with petrophysical constraint only (Inv. FCM), and integration of borehole data in the inversion (Inv. FCM + BH). The borehole data is smoothed by a low-pass filter.

Our inverted model is more comparable with inverted seismic impedance data than the smooth inversion results. The acoustic impedance (AI) section (Figure 11a) derived by a model-based inversion algorithm (performed independently) shows very similar features to our MT models. However, to make the seismic impedance inversion workable, the same borehole information is used. The orebody may be reflected in the zones that show a high variation of AI. The resistive zone C in the MT data is consistent with high AI values, and low values of AI zone reflect conductive zone D.

In comparison with borehole resistivity data (Figure 12), our results are closer to the borehole data than the results of the smooth inversion. The inversion result Inv. ModEm could not recover the ‘blocky’ model, but our routine can construct a model with different units that may better represent crystallized media like in the case of Kevitsa.

As a final step, the inversion results of both MT and seismic data can be combined and clustered in the FCM program; the output is a cluster map of the data section (Figure 13). This map can be used like a pseudo-lithological section, whose geological interpretation is much more intuitive than analyzing sections of petrophysical properties (e.g., seismic or MT data) alone.

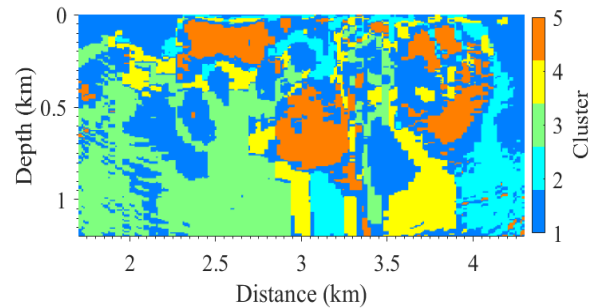


Figure 13: Cluster results using both acoustic impedance from 3D seismic and resistivity from MT in the Inv. FCM+BH model. This cluster model may be used as a pseudo-lithology section to make geophysical data more interpretable than the sections of inverted physical properties alone. Often, a small contrast in physical properties can reflect significant changes in lithology; thus a cluster model provides a useful product in understanding the geology.

CONCLUSIONS

Constraining magnetotelluric inversion via fuzzy clustering provides a powerful tool to include both spatial and petrophysical data to construct a reliable geo-electrical model. Fuzzy c-means guided inversion is shown to separate the major geo-electrical rock units, differentiating between the highly conductive zones from the other resistive media in MT. The sharper variations between resistive zones better reflect the rock units compared to a smooth resistivity model using a traditional non-linear conjugate gradient inversion method with smoothness constraints. The application of our method to the case study at the Kevitsa mine site shows that our results are comparable, within the resolution limits of MT methods, with known geological models and seismic results. Also, they are consistent with the borehole data. We further note that the cluster models may themselves be used as an interpretation aid, rather than using inverted physical values from the geophysical data.

ACKNOWLEDGEMENTS

We would like to thank Seong Kon Lee, Korea Institute of Geoscience and Mineral Resources, Korea for using his 2D MT inversion code in our implementation. The work is supported by the Deep Exploration Technologies Cooperative Research Centre (DET CRC), whose activities are funded by the Australian Government’s Cooperative Research Centre Program. We would like to thank First Quantum Minerals Ltd. and Boliden Company for the use of their comprehensive datasets. This is DET CRC Document 2017/1010.

REFERENCES

- Bezdek, J. C., R. Ehrlich, and W. Full, 1984, FCM: The fuzzy c-means clustering algorithm: *Computers & Geosciences*, 10 (2-3), 191-203.
- deGroot-Hedlin, C. and S. Constable, 1990, Occam's inversion to generate smooth, two-dimensional models from magnetotelluric data: *Geophysics*, 55 (12), 1613-1624.
- Egbert, G. D. and A. Kelbert, 2012, Computational recipes for electromagnetic inverse problems: *Geophysical Journal International*, 189 (1), 251-267.
- Farquharson, C. G., M. R. Ash, and H. G. Miller, 2008, Geologically constrained gravity inversion for the Voisey's Bay ovoid deposit: *The Leading Edge*, 27 (1), 64-69.
- Johnson, T. C., P. S. Routh, T. Clemo, W. Barrash, and W. P. Clement, 2007, Incorporating geostatistical constraints in nonlinear inversion problems: *Water Resources Research*, 43 (10), W10422.
- Kieu, T. D. and A. Kepic, 2015, Seismic impedance inversion with petrophysical constraints via the fuzzy cluster method: *ASEG Extended Abstracts 2015*.
- Kieu, T. D., A. Kepic, and C. Kitzig, 2015, Classification of geochemical and petrophysical data by using fuzzy clustering: *ASEG Extended Abstracts 2015*.
- Kieu, D. T., A. Kepic, and V. A. C. Le, 2016a, Fuzzy clustering constrained magnetotelluric inversion-case study over the Kevitsa ultramafic intrusion, northern Finland: Presented at Near Surface Geoscience 2016-First Conference on Geophysics for Mineral Exploration and Mining, Barcelona.
- Kieu, D. T., A. Kepic, and A. M. Pethick, 2016b, Inversion of magnetotelluric data with fuzzy cluster petrophysical and boundary constraints: *ASEG Extended Abstracts 2015*.
- Lee, S. K., H. J. Kim, Y. Song, and C.-K. Lee, 2009, MT2DInvMatlab—A program in MATLAB and FORTRAN for two-dimensional magnetotelluric inversion: *Computers & Geosciences*, 35 (8), 1722-1734.
- Lelièvre, P. G., D. W. Oldenburg, and N. C. Williams, 2009, Integrating geological and geophysical data through advanced constrained inversions: *Exploration Geophysics*, 40 (4), 334-341.
- Li, Y. and D. W. Oldenburg, 2000, Incorporating geological dip information into geophysical inversions: *Geophysics*, 65 (1), 148-157.
- Malehmir, A., C. Juhlin, C. Wijns, M. Urosevic, P. Valasti, and E. Koivisto, 2012, 3D reflection seismic imaging for open-pit mine planning and deep exploration in the Kevitsa Ni-Cu-PGE deposit, northern Finland: *Geophysics*, 77 (5), WC95-WC108.
- Ogaya, X., J. Alcalde, I. Marzán, J. Ledo, P. Queralt, A. Marcuello, D. Martí, E. Saura, R. Carbonell, and B. Benjumea, 2016, Joint interpretation of magnetotelluric, seismic and well-log data in Hontomín (Spain): *Solid Earth*, 7, 943-958.
- Paasche, H., J. Tronicke, K. Holliger, A. G. Green, and H. Maurer, 2006, Integration of diverse physical-property models: Subsurface zonation and petrophysical parameter estimation based on fuzzy c-means cluster analyses: *Geophysics*, 71 (3), H33-H44.
- Sasaki, Y., 1989, Two-dimensional joint inversion of magnetotelluric and dipole-dipole resistivity data: *Geophysics*, 54 (2), 254-262.
- Steel, M. A., 2011, *Petrophysical modelling using self-organising maps*: MSc thesis, Curtin University.
- Sun, J. and Y. Li, 2011, *Geophysical inversion using petrophysical constraints with application to lithology differentiation*: 81st Annual International Meeting, SEG, Expanded Abstracts, 2644-2648.